

Deep Learning Guided Undersampling Mask Design for MR Image Reconstruction

Shengke Xue, Ruiliang Bai, and Xinyu Jin

Abstract—***. Hereby, this paper proposes ***

Index Terms—***, ***, ***, ***, ***.

I. INTRODUCTION

MAGNETIC Imaging is ...
The major contributions of this paper include:

- DW-TNNR deploys ***.
- DW-TNNR***.
- This paper designs ***

The remainder of this paper is organized as follows. Section II introduces the related work. Section III exhibits the concrete framework of DW-TNNR, comprising the elaborate optimization procedures. Experimental results offered in Section ?? evaluate the performance of our algorithm. Section IX states the conclusions.

II. RELATED WORK

My previous work of image super-resolution [1], [2].

III. PROBLEM FORMULATION

A. 2D Poisson Mask

Fig. 1 shows the traditional 2D Poisson masks with undersampling from 10% to 40%.

B. 1D Mask

IV. METHOD

A. Network Design

Fig. 2 illustrates the overall architecture of our network. We use MR image data from k -space as input, where we combine real part and image part as two channels. Note that k -space data have been shifted, so that the LF part is located at the geometrical center of frequency images. PMask2D layer denotes the undersampling operation in k -space, where the mask is the trainable parameters. IFFT2D denotes the inverse 2D fast Fourier transformation. Then, we adopt a commonly-used VDSR to reconstruct MR images.

Corresponding author: Shengke Xue (xueshengke@zju.edu.cn)

S. Xue and X. Jin are with the College of Information Science and Electronic Engineering, Zhejiang University, Hangzhou, P. R. China (e-mail: xueshengke@zju.edu.cn; jinxy@zju.edu.cn).

R. Bai are with the *****, Zhejiang University, Hangzhou, P. R. China (e-mail: *****@zju.edu.cn)

This work was supported by the National Natural Science Foundation of China (No. 81873894).

Manuscript received *** **, 2020; revised *** **, 2020.

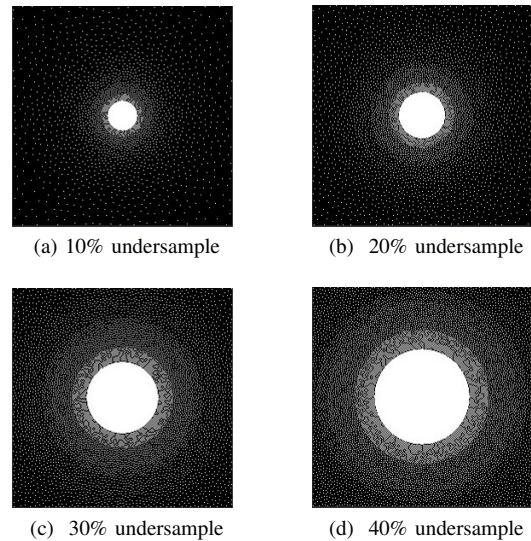


Fig. 1. Examples of Poisson mask from 10% to 40% undersampling

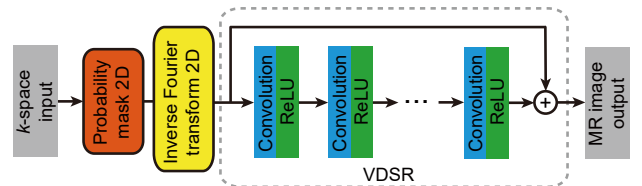


Fig. 2. Framework of our network. Input: k -space MR data; Probability mask 2D: downsampling operation; Output: reconstructed MR image

B. Probability Mask Layer

We define a specialized probability mask layer, to execute the downsampling operator. We use “fft” to achieve the inverse transform from k -space to tempo-spatial space.

Though numerous studies about image super-resolution have been exploited, we choose only a typical CNN-based method, VDSR in our network. Since this paper focuses on discovering the underlying pattern in undersampling mask of k -space, we do not adopt state-of-the-art methods here.

V. EXPERIMENTS

We publish our source code¹ available online. It is based on Tensorflow [3] with Keras API. Matlab is also used to visualize the images. Our experiments are executed on a Ubuntu Linux Server, equipped with an Intel(R) Xeon(R) Platinum CPU @

¹<https://github.com/xueshengke/...-keras>

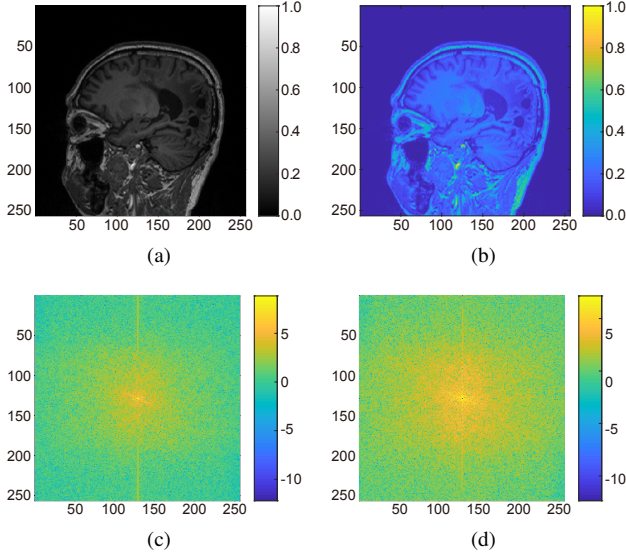


Fig. 3. Example of an MR image and its Fourier representation: (a) gray MR image; (b) color MR image; (c) real part; (d) image part

2.50 GHz, 528 GB memory, and four NVIDIA Tesla V100 (32 GB) GPUs.

A. Datasets

We adopt the 3T brain magnetic resonance images throughout our experiments. It contains 10 samples, each of which comprises a group of 192 IMA-format images with size $256 \times 256 \times 1$. We split 5% of them for validation, the rest for training. Note that the transform error of 2D FFT relies on the image size, we decide not to crop MR images to small patches. Data augmentation scheme is used to prevent over-fitting and boost the generalization capability of our model. Generally, we focus only on the human tissue regardless the background. First, we shift the content to the geometrical center of an MR image, so as to avoid the border effect by the FFT. Then each image is rotated eight times with random angles, since MR images usually have one fixed direction, which are not abundant for training. Since we take the k -space data as the input, we first transform them to the Fourier domain by the 2D FFT function, then we combine the real and image parts of an image as two channels. Example of an MR image and its Fourier representation are illustrated in Fig. 3. Because our model performs image reconstruction, MR images themselves are naturally the ground-truth during training.

B. Evaluation Metrics

Peak signal-to-noise ratio (PSNR) has been commonly used to evaluate the quality of reconstructed images in various computer vision tasks. Literally, PSNR is defined as follows:

$$\text{MSE} = \frac{1}{N} \|I_{\text{SR}} - I_{\text{HR}}\|_F^2, \quad (1)$$

$$\text{PSNR} = 10 \cdot \log_{10} \left(\frac{P_{\max}^2}{\text{MSE}} \right) \text{ dB}, \quad (2)$$

where P_{\max} is the maximum pixel value (normally 1.0) in an image. Additionally, we adopt the structural similarity index

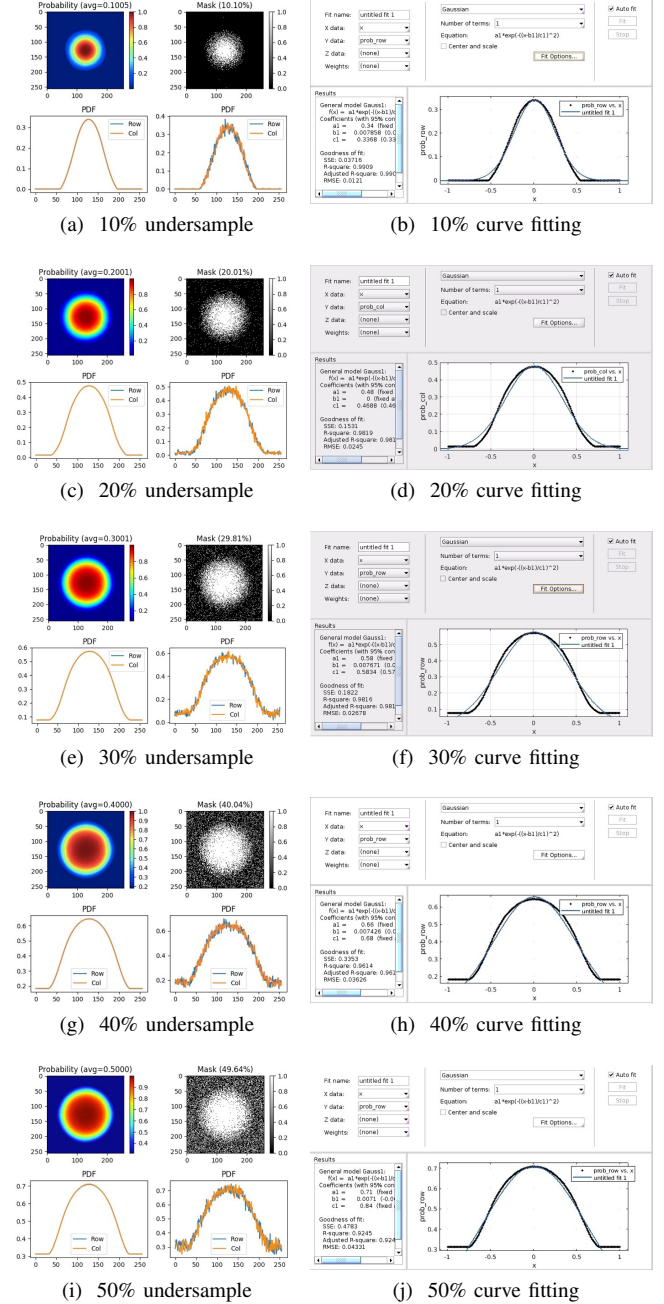


Fig. 4. Examples of probability masks and their corresponding curve fitting results from 10% to 50% undersampling

(SSIM) [4] to access the effect of super-resolution. Its range is $[0, 1]$, where higher value indicates better.

VI. LOSS COMPARISON

IFT loss,
Recover loss,
frequency loss,

VII. RESULTS

VIII. ANALYSIS

Note that all probability masks are discrete, but we use continuous functions to analyze them for simplicity.

TABLE I
QUANTITATIVE RESULTS OF RECONSTRUCTED MR IMAGES BY PROB MASK LAYER AND VDSR-10 UNDER DIFFERENT UNDERSAMPLING RATES

Undersampling rate	IFT PSNR (dB) / Rec PSNR (dB)				
	Poisson mask	Prob mask (with CNN)	Syn mask (with CNN)	Prob mask (no CNN)	Syn mask (no CNN)
10%	32.21 / 35.95	34.25 / 37.34	/	32.80 / -	/ -
20%	34.26 / 38.13	37.93 / 41.15	/	36.98 / -	/ -
30%	36.53 / 40.44	40.70 / 43.46	/	39.06 / -	/ -
40%	39.22 / 42.00	40.99 / 44.87	/	41.06 / -	/ -
50%	41.42 / 44.66	42.01 / 45.92	/	44.54 / -	/ -

TABLE II
COMPARISON OF QUANTITATIVE RESULTS OF DIFFERENT DEPTHS OF VDSR TRAINED MR IMAGES BY PROB MASK LAYER UNDER DIFFERENT UNDERSAMPLING RATES

Undersampling rate	IFT PSNR (dB) / Rec PSNR (dB)		
	VDSR-5	VDSR-10	VDSR-20
10%	- / -	34.25 / 37.34	- / -
20%	- / -	37.93 / 41.15	- / -
30%	- / -	40.70 / 43.46	- / -
40%	- / -	40.99 / 44.87	- / -
50%	- / -	42.01 / 45.92	- / -

TABLE III
PARAMETERS FROM EXPERIMENTAL WITH VDSR, OBTAINED BY THE CURVE FITTING TOOL

r	σ	t	$G(t)$
0.1	0.2317	\pm	0.0399
0.2	0.3182	\pm	0.0798
0.3	0.4101	\pm	0.1197
0.4	0.5006	\pm	0.1596
0.5	0.5719	± 0.7851	0.1995

A. Curve Fitting

We assume the probability density function is a variant of Gaussian distributions, i.e.,

$$G(x|r, \mu, \sigma) = \frac{2r}{\sqrt{2\pi}\sigma} \exp\left(-\left(\frac{x-\mu}{\sqrt{2}\sigma}\right)^2\right), \quad (3)$$

where r is the undersample rate, μ is the mean value, and σ is the deviation. For simple notations, we set $\mu = 0$ and normalize the positions of mask to $[-1, 1]$. Following the integral property of the Gaussian function, we obtain

$$\int_{-\infty}^{+\infty} G(x|r, \sigma) dx = 2r. \quad (4)$$

However, in our case, the undersampling interval is limited between $[-1, 1]$. This leads to the actual undersampling rate smaller than $2r$:

$$\int_{-1}^{+1} G(x|r, \sigma) dx < 2r. \quad (5)$$

To keep the real undersampling rate equal to the pre-set value, we assume that there is a minimum constraint to compensate this loss. Thus, we define

$$U(x) = \theta, \quad x \in [-1, 1]. \quad (6)$$

Provided that $G(x)$ and $U(x)$ cross at $x = \pm t$ ($t < 1$), we compute the corrected undersampling rate through the integral area from $[-1, 1]$ as follows:

$$\int_{-1}^{-t} U(x) dx + \int_{-t}^t G(x) dx + \int_t^1 U(x) dx = 2r. \quad (7)$$

Since $G(x)$ and $U(x)$ are both even functions, (7) can be simplified as

$$2 \int_0^t G(x) dx + 2 \int_t^1 U(x) dx = 2r. \quad (8)$$

Together with the property $U(t) = \theta = G(t)$, we can obtain

$$t = \sqrt{-2\sigma^2 \log_e \left(\frac{\sigma}{2}\right)}, \quad (9)$$

which indicates that t is proportional only to σ (not r). In another word, as σ becomes larger, i.e., $G(x)$ becomes wider, t approaches to 1.

Taking (9) into (3), we obtain

$$G(t) = \theta = \frac{r}{\sqrt{2\pi}}, \quad (10)$$

which means the minimum undersampling rate can be directly determined by the real undersampling rate itself.

B. Mask Design

C. Effect of VDSR on generating mask

We conduct some experiments to verify the effectiveness of VDSR on generating the 2D probability mask. With or without CNN after the 2D IFFT layer to further improve the quality of reconstructed images, the patterns generated in the masks are quite different.

As Fig. 5 shows, the probability density functions under various undersampling rate are almost similar to quadratic functions. Thus, we presume

$$Q(x) = -ax^2 + bx + c, \quad a > 0, \quad (11)$$

where $b = 0$ is confirmed in our case. Following the same assumption in Section VIII-A, we introduce a minimum constraint to keep the actual undersampling rate consistent to the expected value. Assume that $Q(t)$ is the minimum value in the probability density function, we have

$$\int_{-1}^{-t} Q(t) dx + \int_{-t}^t Q(x) dx + \int_t^1 Q(t) dx = 2r, \quad (12)$$

$$2 \int_0^t Q(x) dx + 2 \int_t^1 Q(t) dx = 2r. \quad (13)$$

$$\frac{2}{3} at^3 - at^2 + c = r. \quad (14)$$

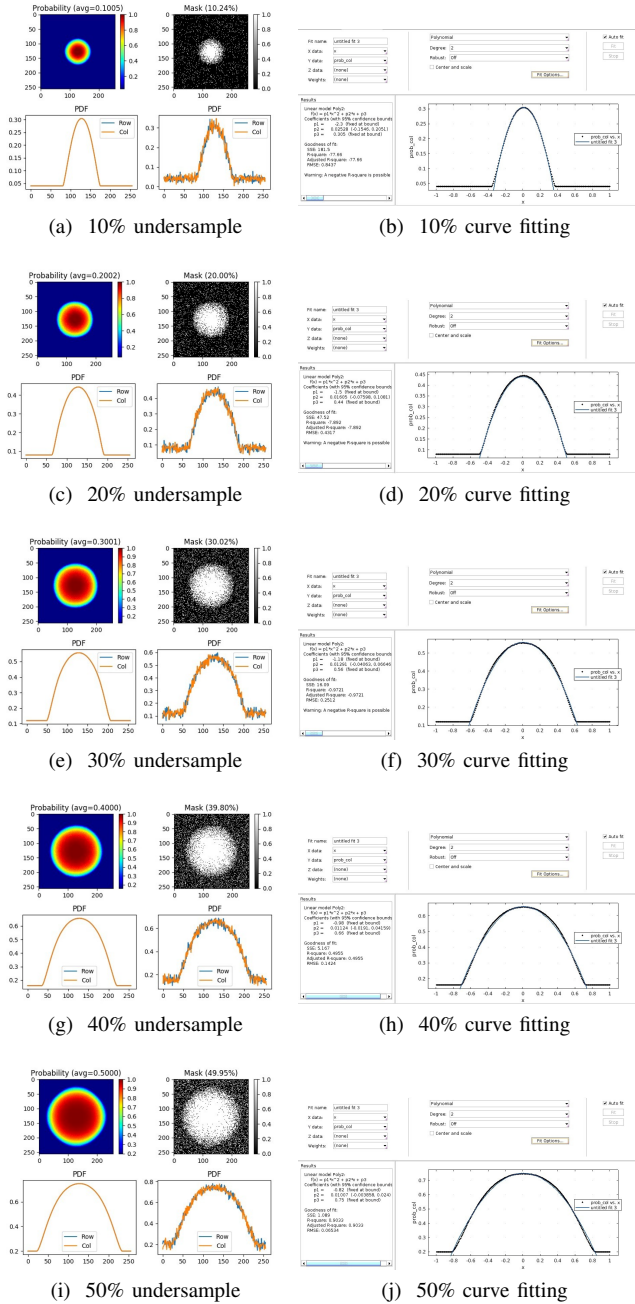


Fig. 5. Examples of probability masks and their corresponding curve fitting results w/o VDSR from 10% to 50% undersampling

Following the same property of (3) and (10), we obtain

$$Q(t) = -at^2 + c = \frac{r}{\sqrt{2\pi}}. \quad (15)$$

According to the results of the curve fitting tool in Matlab (Fig. 6), we discover that

$$a \propto \frac{r}{\sigma^4}, \quad c \propto \frac{r}{\sigma}. \quad (16)$$

Together with (14), (15), and (16), we can solve

$$a = \frac{r}{3\sqrt{2\pi}\sigma^4}, \quad c = \frac{2r}{\sqrt{2\pi}\sigma}. \quad (17)$$

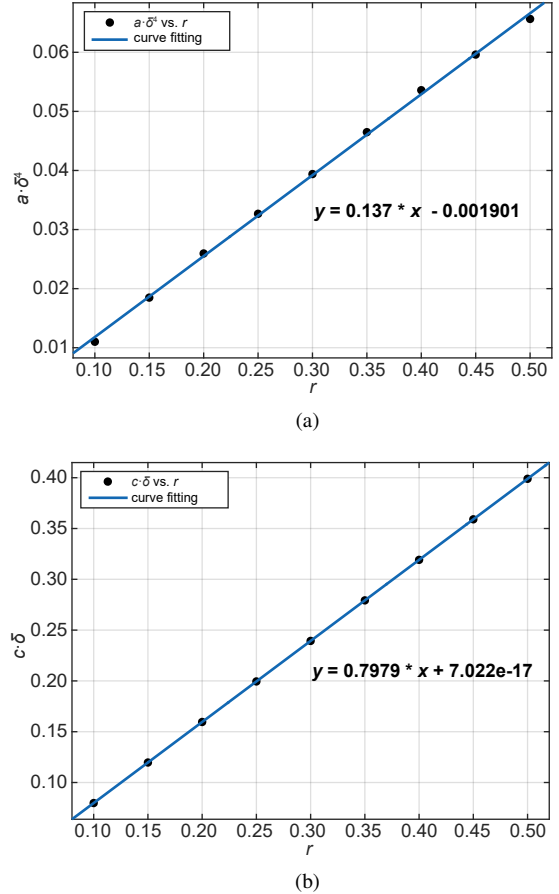


Fig. 6. Curve fitting results: $a \cdot \sigma^4$ vs. r is linear; $c \cdot \sigma$ vs. r is linear

TABLE IV
PARAMETERS FROM TRAINED MODEL WITHOUT VDSR, BY THE CURVE FITTING TOOL

r	a	c	σ	t	$G(t)$
0.1	-2.20	0.30	0.2660	0.3434	0.0406
0.2	-1.50	0.44	0.3627	0.4867	0.0847
0.3	-1.18	0.56	0.4274	0.6091	0.1223
0.4	-0.98	0.66	0.4836	0.7095	0.1666
0.5	-0.82	0.75	0.5319	0.8202	0.1984

Finally, the probability mask without VDSR reconstruction has a different function:

$$G(x) = -\frac{r}{3\sqrt{2\pi}\sigma^4}x^2 + \frac{2r}{\sqrt{2\pi}\sigma}. \quad (18)$$

So far, we have discovered two universal probability density functions for generating probability mask to achieve k -space undersampling. They are quite different from existing mask patterns, e.g., Poisson disc mask.

IX. CONCLUSION

In this paper, we have proposed ...

APPENDIX A

APPENDIX B

APPENDIX C

REFERENCES

- [1] S. Xue, W. Qiu, F. Liu, and X. Jin, "Faster image super-resolution by improved frequency-domain neural networks," *Signal, Image and Video Processing*, vol. 14, p. 257265, Aug 2020.
- [2] S. Xue, W. Qiu, F. Liu, and X. Jin, "Wavelet-based residual attention network for image super-resolution," *Neurocomputing*, vol. 382, pp. 116–126, Dec 2019.
- [3] M. Abadi, P. Barham, J. Chen, and et al., "Tensorflow: a system for large-scale machine learning," in *12th USENIX Symp. on Operating Systems Design and Implementation*, 2016, pp. 265–283.
- [4] Z. Wang, A. Bovik, H. Sheikh, and E. Simoncelli, "Image quality assessment: from error visibility to structural similarity," *IEEE Trans. Image Process.*, vol. 13, no. 4, pp. 600–612, apr 2004.